Online-Journals.org

iJOE International Journal of Online and Biomedical Engineering

iJOE | eISSN: 2626-8493 | Vol. 21 No. 10 (2025) | OPEN ACCESS

https://doi.org/10.3991/ijoe.v21i10.56201

PAPER

Beta Wavelet Neural Networks for Medical Image Watermarking: A Fast and Robust Approach

Rayen Ben Salah (✉), **Mourad Zaied**

Research Team in Intelligent Machines, National Engineering School of Gabes, University of Gabes, Gabes, Tunisia

rayen.bensalah@isimg.tn

ABSTRACT

Smart devices and modern communication technologies now connect medical equipment more easily, which helps improve diagnostic processes. These systems use medical images to support diagnosis and decision-making, so it's important to protect those images. Digital watermarking offers an effective way to secure medical images by embedding information that can verify authenticity, protect copyright, and ensure traceability throughout the healthcare workflow. To address this issue, this paper presents a robust and efficient medical image watermarking scheme that integrates the fast Beta wavelet transform (FBWT) with wavelet neural networks (WNN). Firstly, we created a library of activation functions containing a newly introduced family of Beta wavelets. Secondly, leveraging multi-resolution analysis (MRA) and fast wavelet transform (FWT), the medical image was decomposed to obtain wavelet coefficients. Finally, this approach embeds a watermark within the least significant contributions of the host medical image using WNN while maintaining high imperceptibility and robustness. Experimental results demonstrate the effectiveness of the scheme in balancing invisibility and resilience against various attacks, making it a promising solution for securing medical images in telemedicine applications. For imperceptibility evaluation, we used the peak signal-to-noise ratio (PSNR) and the structural similarity index measure (SSIM), with values of PSNR = 81.49 and SSIM = 1.000. In robustness testing, we measured the normalized correlation (NC) and bit error rate (BER), obtaining values of NC = 1.000 and BER = 0.

KEYWORDS

watermarking, medical image, Beta wavelet, fast wavelet transform (FWT), wavelet neural networks (WNN)

1 INTRODUCTION

Telemedicine has advanced significantly with the evolution of the internet and communication technologies, enabling clinicians and patients to exchange medical images and other healthcare data efficiently. However, this digital transmission raises critical concerns about intellectual property protection and data security.

Salah, R. B., Zaied, M. (2025). Beta Wavelet Neural Networks for Medical Image Watermarking: A Fast and Robust Approach. *International Journal of Online and Biomedical Engineering (iJOE)*, 21(10), pp. 94–108. https://doi.org/10.3991/ijoe.v21i10.56201

Article submitted 2025-04-23. Revision uploaded 2025-06-19. Final acceptance 2025-06-19.

Digital watermarking provides a promising solution by embedding authentication or ownership information directly in medical images. This approach helps ensure both the confidentiality of patient data and the integrity of medical records while maintaining acceptable visual quality. Based on the notion of embedding information, watermarking algorithms can be classified into spatial domain methods [1], [2], [3], [4] and transform domain methods [5], [6], [20], [7].

The first type's techniques embed data directly within the pixel values of the cover image, often targeting the least significant bits to preserve the visual quality. Examples of such methods include LSB, spread spectrum, CDMA, and the work approach. In contrast, transform domain techniques are more commonly used and work by embedding watermark data in the image's spectral coefficients. Popular transform domain techniques include the discrete cosine transform (DCT), discrete Fourier transform (DFT), singular value decomposition (SVD), discrete wavelet transform (DWT), Hadamard transform (HT), and Contourlet transform (CT). Insertion of the secret data is generally easier in the spatial domain watermarking compared to the transform domain. However, transform domain watermarking offers greater robustness than spatial watermarking [8]. Traditional watermarking techniques often depend on fixed wavelet bases and manually selected parameters, which can limit their effectiveness, especially when handling the high variability and complexity of medical images. To overcome these limitations, this work introduces a watermarking method based on wavelet neural networks (WNNs). By combining the learning capabilities of neural networks with the multiresolution properties of wavelets, WNNs enable adaptive, robust, and imperceptible watermark embedding tailored to the image's characteristics. The integrated wavelets are part of a newly introduced wavelet family called Beta wavelets.

The contributions we provided are highlighted in the following approach:

- Creating a library of scaling and wavelet functions built from a mother Beta wavelet.
- Computing the coefficients of the wavelet and scaling functions to determine the least significant contributions in the cover image through the WNN, this will be used as positions for embedding the watermark.
- Reconstructing the watermarked medical image and extracting the watermark to evaluate the experimental results to balance the image's imperceptibility and robustness.

This paper is divided into the following sections: Section 2 presents an overview of the related works. Section 3 presents the concepts of multiresolution analysis (MRA), Beta wavelets, WNNs, and fast wavelet transform (FWT). Section 4 details the steps of our methodology. Section 5 reports the experimental results, provides their analysis, and compares them with other approaches. Section 6 presents the limitations of the proposed method and future work. Finally, Section 7 provides the conclusion of the work.

2 RELATED WORKS

This section reviews previous studies on robust digital image watermarking techniques. These methods safeguard private content by ensuring resilience against attacks. Methods differ according to the techniques used for insertion and extraction of the data. Using transform domain techniques, we can see that Amsaveni et al. in

their study [5] proposed a watermarking technique for medical images that uses the Radon and Slantlet transforms. First, the cover image is transformed from the spatial domain to the Radon domain, where rotation, scaling and translation change the positions of the hidden bits. This makes it difficult to detect the embedded data without applying the inverse Radon transform. Then, the Radon-transformed image is shifted to the frequency domain using the Slantlet transform. The secret bits are embedded into the frequency coefficients by applying the pixel pair mapping method. Finally, the watermarked image is created by embedding the side information into the robust watermarked version. Building on this concept of combining multiple transforms for enhanced security and robustness, another approach introduces a different set of frequency domain techniques tailored for medical imaging. This study [6] integrated the fractional discrete cosine transform (FDCT), radon transform, and Schur decomposition techniques to insert the watermark. The methodology specifically aims at low-frequency coefficients containing essential structural and illumination information for watermark embedding, thereby maintaining robustness and visual transparency. However, this approach may face difficulties in extracting the watermark reliably under changing conditions, and it still needs to be tested on various types of medical images to confirm its clinical usefulness. Laouamer et al. [9] proposed a watermarking method for medical images based on the Hough transform that detects line segments used as embedding targets. Lines are identified using their (θ, ρ) parameters to select relevant regions and reduce computation. The watermark is generated from the peaks of the detected lines and embedded on the corresponding pixels using linear interpolation. A visibility parameter δ controls transparency, with values close to 1 improving invisibility. The watermark extraction involves re-detecting lines and reversing the embedding. The method achieves high imperceptibility (average PSNR of 65 dB) and robustness (correlation coefficients close to 1), although it can be computationally intensive and requires more extensive testing on diverse medical image datasets.

As a complementary direction to transform-based techniques, some approaches integrate cryptographic tools to enhance security, especially for the protection of sensitive medical data. In [10], the authors propose a watermarking method for encrypted medical images that combines multi-level DWT, the Daisy descriptor and DCT. First, the image is encrypted using DWT-DCT and logistic mapping. Then they apply three levels of DWT and select the center of the LL3 sub-band as the key sampling point. At this point, they compute the Daisy descriptor, and transform it using DCT. A perceptual hash is applied to the result to generate a 32-bit binary feature vector. This method uses zero watermarking, which means that the watermark is associated with the image features without modifying the image itself.

With the growing capabilities of deep learning, recent methods have begun to use neural networks to improve the accuracy, adaptability and automation of watermarking for medical image protection. Amrit et al. [11] proposed a dual watermarking technique for medical images using ConvNet-HIDE. They used a customized UNet3+ model to segment medical images into regions of interest (ROI) and non-ROI, combined with MobileNetv2 for feature extraction and pix2pix-based up sampling. This segmentation enables precise watermark embedding. Two watermarks are embedded using the Mobi-ConvNet model, minimizing distortion and improving security. The extraction process uses a ConvNet model and principal component analysis (PCA) for reliable watermark recovery. However, the method struggles to balance robustness, imperceptibility, and embedding capacity compared to simpler single watermarking techniques.

However, previous methods often face problems. They do not handle strong attacks well, struggle to keep the watermark consistent across different image formats, and are rarely tested in clinical settings. To address these issues, we combine the FWT

with WNN. This approach allows for multi-level image analysis and detail localization. To the best of our knowledge, our method is the first to use Beta wavelet neural networks to embed and extract watermarks while keeping them both invisible and robust.

3 TECHNICAL BACKGROUND

To ensure the robustness and effectiveness of the proposed watermarking method, it is essential to rely on strong mathematical tools and signal processing techniques. This section presents the theoretical foundations underlying our approach, including multiresolution analysis, wavelet neural networks, and the use of Beta wavelets and fast wavelet transform.

3.1 Multiresolution analysis

Wavelet theory enables the analysis of signals through a multi-resolution structure, applicable to both discrete and continuous time domains. This MRA decomposes signals into components at varying resolutions, organizing them into subspaces, each representing an approximation at a specific scale. The scaling function $\phi(x, y)$ approximates the signal, while wavelet functions $\psi(x, y)$ capture the differences between successive approximations.

In 2D images, this results in four sub bands: one approximation (LL) and three detail bands, horizontal (HL), vertical (LH), and diagonal (HH) using coefficients V, W^H,W^V, and, W^D respectively [12]. The relationships between these wavelets are defined as equations (1), (2), (3), and, (4).

$$\phi(x, y) = \phi(x)\ \psi(y) \tag{1}$$

$$\psi^H(x, y) = \phi(x)\psi(y) \tag{2}$$

$$\psi^V(x, y) = \psi(x)\phi(y) \tag{3}$$

$$\psi^D(x, y) = \psi(x)\psi(y) \tag{4}$$

The transformation functions for scaling and wavelets are represented as equations (5) and (6).

$$\phi_{m,n_x,n_y}(x, y) = 2^{\left(-\frac{m}{2}\right)}\phi(2^{-m}x - n_x, 2^{-m}y - n_y) \tag{5}$$

$$\psi^i_{m,n_x,n_y}(x, y) = 2^{\left(-\frac{m}{2}\right)}\psi(2^{-m}x - n_x, 2^{-m}y - n_y), i \in \{H, V, D\} \tag{6}$$

With m is the scale level, and n_x, n_y are the translation indices.

Decomposition phase. The 2D multiresolution wavelet framework extracts the scaling coefficients V and the directional detail coefficients $\boldsymbol{W^i}$ using dual scaling and wavelet functions $(\tilde{\boldsymbol{\phi}}, \tilde{\boldsymbol{\psi}})$ during the analysis phase and primal functions $(\boldsymbol{\phi}, \boldsymbol{\psi})$ during the reconstructing phase [13]. These coefficients are defined in equations (7) and (8).

$$V_{m,n_x,n_y} = \frac{1}{\sqrt{MN}}\sum_{x=0}^{M-1}\sum_{x=0}^{N-1} f(x, y)\tilde{\phi}_{m,n_x,n_y}(x, y) \tag{7}$$

$$W^{i}_{m,n_x,n_y} = \frac{1}{\sqrt{MN}} \sum_{x=0}^{M-1} \sum_{x=0}^{N-1} f(x,y) \tilde{\psi}^{i}_{m,n_x,n_y}(x,y), i \in \{H,V,D\} \tag{8}$$

With m is the scale level, and n_x, n_y are the translation indices.

Reconstruction phase. The signal reconstruction integrates approximation and detail components as mentioned in equation (9).

$$f(x,y) = \sum_{x=0}^{N-1} V_{m,n_x,n_y}, \phi_{m,n_x,n_y} + \sum_{x=0}^{M-1} \sum_{x=0}^{N-1} W^{i}_{m,n_x,n_y}, \psi^{i}_{m,n_x,n_y}(x,y), i \in \{H,V,D\} \tag{9}$$

3.2 Beta wavelet family

Beta wavelets represent an innovative and parametric approach to signal analysis. These wavelets are built on the unique properties of the Beta function developed by [14]; its equation is given by (10).

$$\beta(x,p,q,x_0,x_1) = \begin{cases} \left(\frac{x-x_0}{x_c-x_0}\right)^p \left(\frac{x_1-x}{x_1-x_c}\right)^q & if\ x \in [x_0,x_1] \\ 0 & else \end{cases} \tag{10}$$

where p, q, x_0 *and* $x_1 \in \mathbb{R}$, $x_0 < x_1$ and $x_c = \frac{(px_1 + qx_0)}{(p+q)}$.

The derivatives of the Beta function form the basis of orthogonal and biorthogonal wavelet systems. These systems have finite support and oscillatory behavior, and they meet the admissibility condition. Beta wavelets are smooth (infinitely differentiable) and follow the principles of MRA, which allows them to perform multiscale transformations of signals or images [15]. Figure 1 shows an example of a Beta wavelet and its first two derivatives.

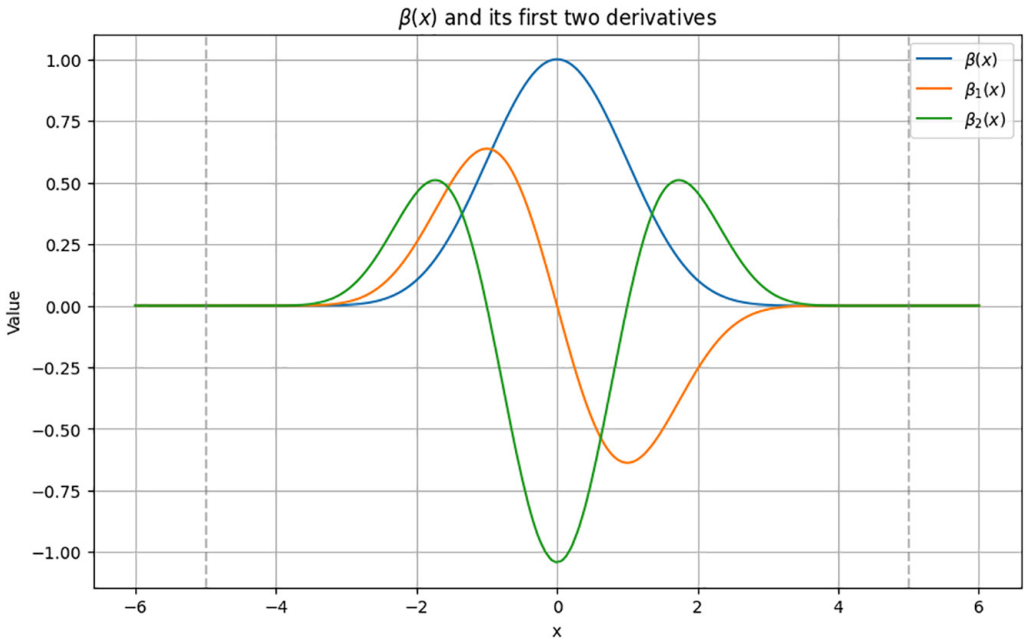

Fig. 1. Beta function and two first derivatives

In comparison with conventional wavelets such as Haar, Daubechies, and Biorthogonal, which exhibit limited flexibility due to their fixed structural properties, Beta wavelets offer a distinct advantage through their parametric design, governed by the shape-controlling parameters α and β. These parameters allow precise adjustment of the wavelet's shape and smoothness, enabling the Beta wavelet to match a wide variety of signal forms ranging from sharp edges to smooth transitions. This inherent flexibility makes Beta wavelets particularly effective for processing complex signals such as medical images, which typically contain both homogeneous regions and abrupt intensity changes. Experimental results confirmed the superiority of Beta wavelets within the proposed fast Beta wavelet transform (FBWT)-based watermarking scheme, achieving a PSNR of 81.49 dB and an SSIM of 1.000, significantly outperforming conventional wavelet-based methods. In another study by Ben Amar et al. [15], Beta wavelets were applied to lossy image compression tasks, where they outperformed standard wavelets such as Haar, Daubechies, and Coiflet in terms of PSNR and mean squared error (MSE), while preserving important image details. Furthermore, Zahmoul et al. [16] introduced a new chaotic encryption scheme based on Beta functions, demonstrating enhanced security features, including high entropy, strong key sensitivity, and superior resistance to statistical and differential attacks, surpassing the performance of traditional chaotic maps.

These studies show that Beta wavelets are adaptable, precise, and robust. They are well-suited for medical image watermarking, where image quality and security are very important.

3.3 Wavelet neural networks

In 1992, Zhang [17] combined wavelet transforms and neural networks to create the theory of wavelet networks, a powerful tool for signal processing and analysis. The method uses a set of wavelets derived from a single mother wavelet, modified by specific weighted translations and dilations. The hidden layer of the wavelet network can include both scaled and translated versions of the mother wavelet's scaling function. This hybrid wavelet network is effective for adaptive representation modeling of MRA of 2D signals. The output of this network is represented by the following formula (11).

$$\tilde{f} = \sum_{i=1}^{n} W_i^k \psi_i + \sum_{j=1}^{m} V_j \phi_j, \; k \in \{H, V, D\} \tag{11}$$

3.4 Fast wavelet transform

The fast wavelet transform is a powerful tool for MRA, combining spatial and frequency information. It decomposes an image into four sub-bands: LL (approximation), HL (horizontal details), LH (vertical details), and HH (diagonal details), and captures both coarse approximations and fine details at different scales [18]. This is done using low-pass and high-pass filters in horizontal and vertical directions. FWT efficiently highlights key image features while reducing computation time. To reconstruct the image, the process is reversed using synthesis filters, gradually combining details and approximations to restore the original with excellent fidelity. Figure 2 illustrates the 2D FWT architecture.

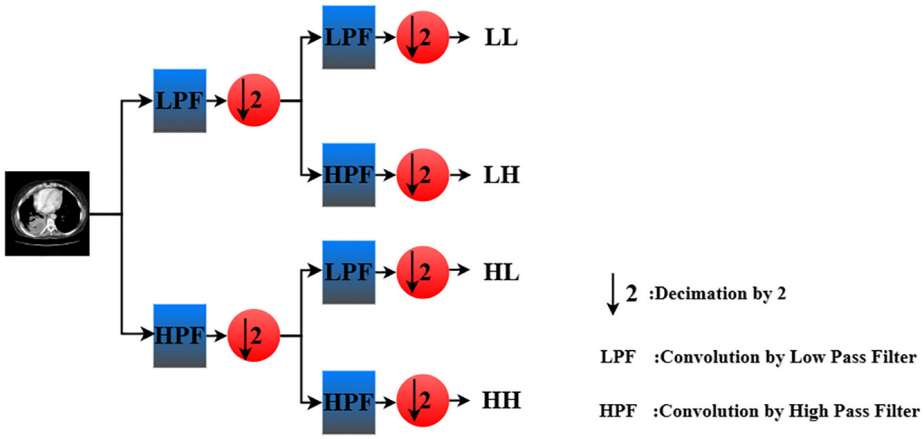

Fig. 2. FWT architecture

4 PROPOSED WATERMARKING SCHEME

Building on the theoretical concepts presented earlier, we now introduce the watermarking scheme. The watermark embedding process includes an adaptive training phase of the WNN, which identifies optimal insertion regions based on the FBWT coefficients without the need for a large-scale training dataset.

4.1 Embedding watermark using FBWT and WNN

To generate the watermarked medical image C^*, a cover image C with size $p = M * M$ and a watermark W with size $q = N * N$ are used. The watermarking process involves the following steps:

- **Step 1: Library initialization:** Develop a library of scaling and wavelet functions, denoted as $g = \{g_1, g_2, ..., g_p\}$. These functions serve as activation functions in the WNN.
- **Step 2:** Specify the number of iterations to be performed.
- **Step 3: Coefficient computation:** Compute the coefficients W_i^H, W_i^V, W_i^D and V_i for the wavelet and scaling functions in the defined library. This is achieved by applying an FBWT to the host image, utilizing a dual set of wavelet and scaling function filters $(\tilde{h}, \tilde{g})$, organized in a list α_p.
- **Step 4: Contribution computation:** Calculate the contribution of all activation functions in the library

$$C_i^H = W_i^H \psi_i^H$$

$$C_i^V = W_i^V \psi_i^V$$

$$C_i^D = W_i^D \psi_i^D$$

$$C_i = V_i \phi_i$$

- **Step 5: Sorting contributions:** Arrange all computed contributions in ascending order based on their magnitude.
- **Step 6: WNN construction:** Develop the WNN, where the output depends on the hidden layer functions and their associated connection weights. The medical

image is then divided into four parts, each containing the least significant contributions. These identified regions represent the suitable positions to embed the watermark, where the input (w_x, w_y) corresponds to the size of the watermark.

- **Step 7: Stopping condition:** Set a stopping criterion where the number of iterations must be divisible by 4. If this condition is not met, return to Step 2.
- **Step 8: Watermark splitting and embedding:** Divide the watermark into four parts, each part into one of the regions containing the least significant contributions, using a scaling factor γ.
- **Step 9: Watermarked image reconstruction:** Reconstruct the watermarked medical image by applying the primary set of functions (ψ, ϕ) using Inverse fast Beta wavelet transform.

Figure 3 illustrates the insertion process of the watermark in the medical image.

Fig. 3. Watermarking embedding architecture

4.2 Extraction watermark using FBWT and WNN

In this process, C^* represents the watermarked image, and W^* is the extracted watermark. The watermark extraction process is semi-blind: while it does not require the original cover image, it does rely on prior knowledge of the activation functions and the scaling factor used during embedding. This ensures accurate extraction of the watermark, but implies that some auxiliary information must be securely shared.

- **Step 1: Library initialization:** Get the same activation functions used in the insertion module.
- **Step 2: Coefficient computation:** Perform FBWT to C^* to get the the coefficients of activation functions using $(\tilde{h}, \tilde{g})$.
- **Step 3: Contribution's computation:** For each activation function, recompute its contribution.

- **Step 4: Sorting contributions:** Sort the contributions in ascending order.
- **Step 5: WNN construction:** Split C^* into four sections, following the same method used during the watermark embedding process. Then, using WNN, extract each segment of the watermark from the least significant contributions by dividing them by the scaling factor γ.

$$W^* = \frac{Worst\ contributions}{\gamma}$$

- **Step 6:** Reconstruct W^*.

4.3 Security of auxiliary information

In practical deployments, the sender and receiver share the required auxiliary data, such as the activation function and scaling factor, during a one-time system initialization phase. These values stay the same for all future sessions; they do not need to be transmitted with each image. This avoids transmission risks and prevents extra data from being embedded in the image. As a result, the image quality remains unaffected, which is crucial in medical imaging to ensure proper clinical interpretation. This approach keeps both security and image integrity intact.

5 EXPERIMENTS AND RESULTS

This section presents the experimental evaluation of the proposed watermarking scheme in terms of imperceptibility and robustness, followed by a comparative analysis against state-of-the-art methods. For every experiment, MATLAB R2021a was used on a PC with an Intel Core i7 CPU clocked at 2.90 GHz and 16 GB of RAM. The watermark embedding and extraction processes each took less than 1 second per image. Figure 4 shows the six different types of medical cover images employed: mammogram (see Figure 4a), iris scan (see Figure 4b), chest CT scan (see Figure 4c), chest X-ray (see Figure 4d), normal brain MRI (see Figure 4e), and abnormal brain MRI (see Figure 4f).

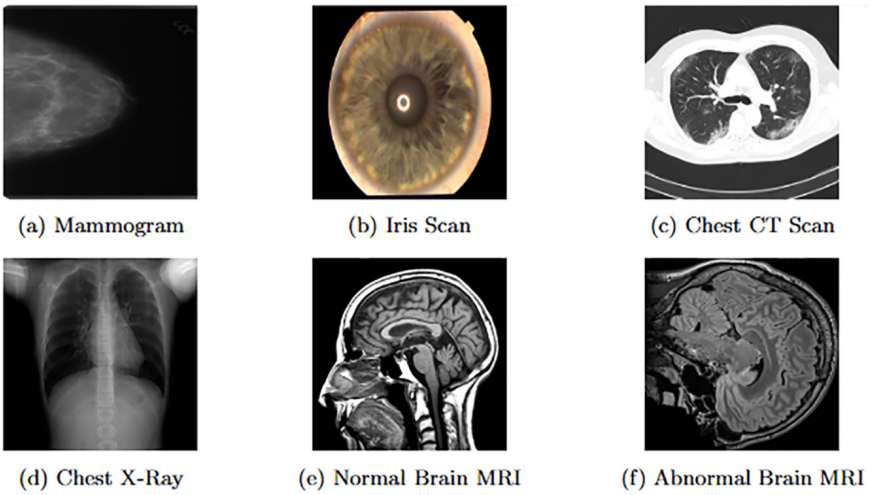

Fig. 4. Cover images

The set of cover images used in this study comprises diverse medical modalities sourced from publicly available datasets. The mammogram image originates from the Breast Tumor Mammography Dataset, which includes high-resolution grayscale

mammograms aimed at breast cancer detection. The iris scan is derived from the Ocular Disease Recognition (ODIR-5K) dataset, which contains fundus images collected from both eyes of 5,000 patients, facilitating research in ocular diagnostics. The chest CT scan image is taken from the Chest CT-Scan dataset, which features annotated CT slices used for lung disease detection. The chest X-ray is obtained from the Chest X-Ray Images (Pneumonia) dataset widely used in pneumonia classification tasks. Lastly, the normal and abnormal brain MRI scans are extracted from the National Library of Medicine's MedPix database, representing healthy and pathological conditions, respectively.

To evaluate the feasibility of the proposed FBWT-WNN watermarking scheme in real-time scenarios, we measured its execution performance on the same computing platform. The embedding and extraction processes required 0.007s and 0.006s per 512×512 image, respectively. These results confirm that the system operates in near-real-time without relying on GPU acceleration or large-scale deep learning model training. To further highlight its computational efficiency, we compared our method with lightweight deep learning-based watermarking approaches such as UNet3+ [11] and Swin-UNet [19]. These methods require 0.022 and 0.013 s per image and often depend on GPU processing.

We evaluated imperceptibility using PSNR and SSIM metrics. Our experimental results consistently demonstrate high PSNR and SSIM values across various types of medical images (CT, MRI, X-ray), confirming the imperceptibility and quality preservation of the watermarked images. As shown in Table 1, PSNR values range from 65.14 dB to 81.49 dB, demonstrating excellent preservation of image quality. SSIM values for most images reach 1.000, confirming the near-perfect visual fidelity of the watermarked images. Higher values of these metrics indicate better image quality.

Table 1. Imperceptibility tests

Tested Images	PSNR	SSIM
Mammogram	81.49	1.000
Iris Scan	73.13	0.999
Chest CT Scan	76.37	1.000
Chest X-Ray	79.04	1.000
Normal Brain MRI	80.01	1.000
Abnormal Brain MRI	65.14	0.999

Table 2 compares the proposed method to several recent watermarking approaches. Our method clearly outperforms in terms of PSNR. Such high values confirm the effectiveness of integrating Beta wavelets and WNN in achieving imperceptible embedding while maintaining medical image fidelity.

Table 2. Imperceptibility comparison with other methods

Studies	[5]	[6]	[9]	[11]	Proposed
PSNR	54.18	38.54	67.59	39.59	81.49

We applied medical-grade compression formats, specifically JPEG-LS and JPEG XR, to three watermarked 2D DICOM slices. These slices were extracted from the 3D volumes of the Bonn Open Pre-surgery MRI Dataset of people with epilepsy and focal cortical dysplasia type II [21]. Although the original dataset provides 3D MRI volumes, 2D slices were selected to reflect typical PACS workflows where individual slices are stored and

processed. The three slices used in this experiment are shown in Figure 5. In this test, compression was applied after watermark embedding. The images were decompressed before extraction. We measured PSNR and SSIM for visual quality. The results, summarized in Table 3, confirm that the proposed method maintains excellent image quality.

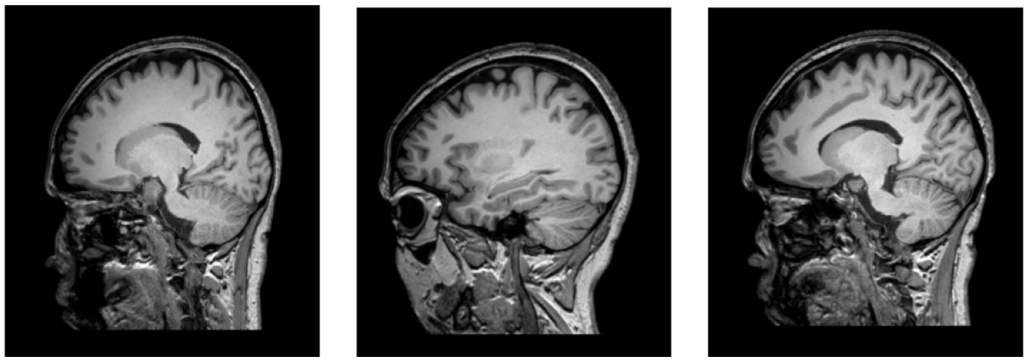

Fig. 5. Dicom images

Table 3. Robustness and visual quality results after JPEG-LS and JPEG XR compression on watermarked images

Compression Format	JPEG-LS (Image1)	JPEGXR (Image1)	JPEG-LS (Image2)	JPEGXR (Image2)	JPEG-LS (Image3)	JPEG-LS (Image3)
PSNR	59.16	46.32	58.41	45.77	58.03	45.32
SSIM	1.000	0.9997	1.000	0.9939	0.9982	0.9921

The robustness evaluation is assessed by subjecting the extracted watermark to various common and geometric attacks. The similarity between the original and extracted watermarks was quantified using Normalized Correlation (NC), while Bit Error Rate (BER) indicates the proportion of incorrectly retrieved bits. As shown in Table 4, the watermark is accurately retrieved under most attacks, with NC values consistently close to 1 and BER values close to 0. Notably, the method is particularly resilient to JPEG compression (QF = 90), Gaussian and Speckle noise, and median filtering.

Table 4. Robustness tests

Attack	NC	BER
No attack	1.000	0
Sharpening	0.9839	0
Histogram equalization	0.9453	0
Motion Blur	0.9918	0
JPEG Compression QF = 50	0.9964	0
JPEG Compression QF = 90	0.9952	0
JPEG2000 Compression CR = 12	0.9754	0
JPEG2000 Compression CR = 50	0.9752	0
Median [9 9]	0.9442	0.804
Median [7 7]	0.9599	0.775

(Continued)

Table 4. Robustness tests *(Continued)*

Attack	NC	BER
Median [5 5]	0.9740	0.682
Median [3 3]	0.9897	0
Gaussian Noise 0.001	0.9990	0
Gaussian Noise 0.01	0.9993	0.069
Speckle Noise 0.001	0.9995	0.075
Speckle Noise 0.01	0.9956	0
Salt and Pepper Noise 0.001	0.999	0
Salt and Pepper Noise 0.01	0.9971	0
Average Filtering [3 3]	0.9935	0
Average Filtering [5 5]	0.9921	0
Average Filtering [7 7]	0.9908	0
Image Scaling 0.25	0.9882	0
Rotation 2	0.9929	0

In comparison with other methods, as shown in figures Figures 6 and 7, the NC values demonstrate that our method consistently outperforms the other techniques, maintaining higher similarity scores across different distortions, including noise addition, filtering, blurring, and compression. Notably, our approach exhibits superior resilience against JPEG compression (QF = 90), salt and pepper noise (0.01), and median filtering, where it achieves significantly higher NC values compared to the other methods. This highlights the effectiveness of our hybrid watermarking technique in preserving the integrity of the watermark under common attacks, making it a more reliable solution for secure medical image protection and copyright enforcement.

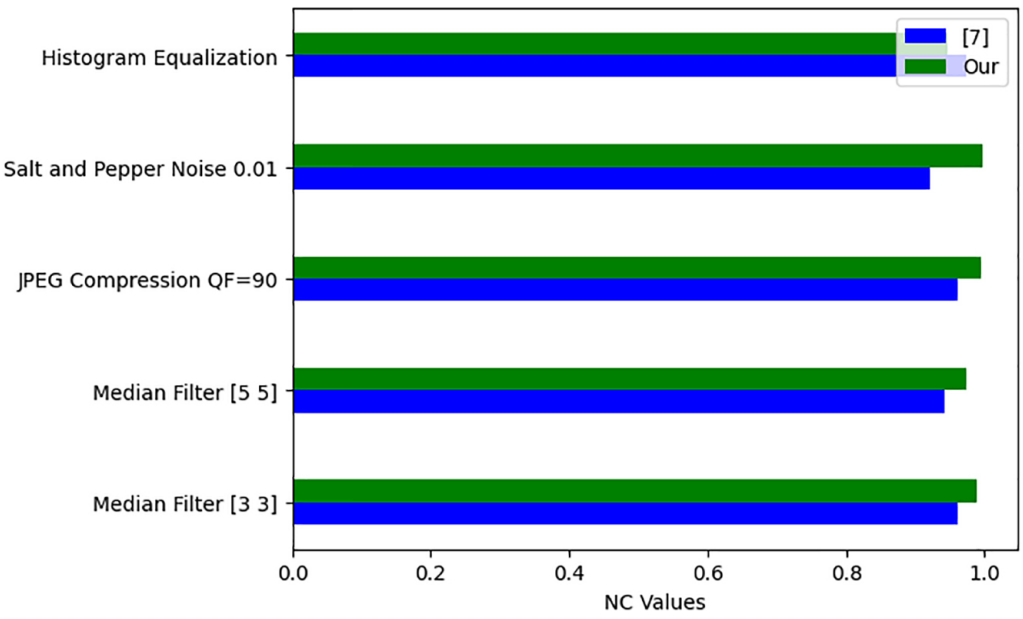

Fig. 6. NC values comparison with reference [7]

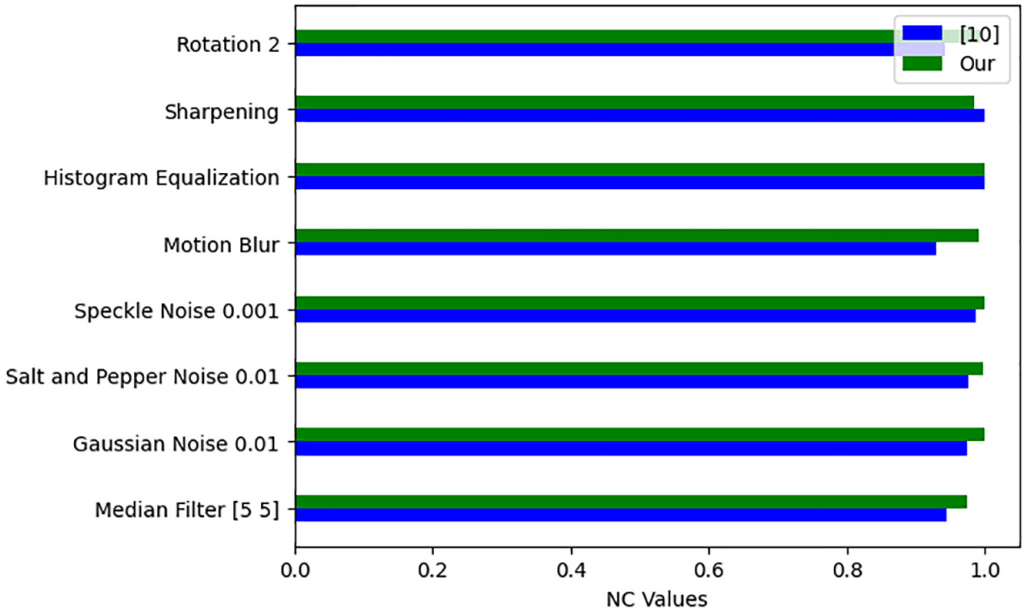

Fig. 7. NC values comparison with reference [10]

6 LIMITATIONS AND FUTURE WORKS

Despite the promising results achieved by the proposed watermarking scheme, several limitations must be acknowledged. The method exhibits some vulnerability to aggressive nonlinear filtering operations such as median filters with large kernel sizes (e.g., 9×9), where the BER significantly increases. This is likely due to the fact that the watermark is embedded in low-magnitude detail regions that are strongly suppressed or modified by such filters. To mitigate this limitation, future work will explore adaptive embedding strategies that select more resilient regions based on local image complexity. Future work will focus on addressing these issues by enhancing the system's robustness to nonlinear distortions and integrating formal security frameworks. In addition, future developments may involve the design of adaptive watermarking strategies incorporating cryptographic features to ensure both integrity verification and traceability in healthcare image workflows.

7 CONCLUSION

This paper introduces a medical image watermarking method based on the FBWT and WNN. The proposed approach ensures excellent visual quality (PSNR up to 81.49 dB) and strong robustness (NC = 1.000, BER = 0), with very little distortion to the original image. It also outperforms several existing techniques, especially under different types of attacks.

One of the main strengths of this work is the use of the Beta wavelet family, which offers a flexible and powerful way to embed watermarks in different frequency bands. This makes the method particularly suitable for protecting the integrity of medical images, especially in remote diagnostics and secure healthcare systems. Although the results are promising, the experimental evaluations confirm the method's suitability for near-real-time applications on standard CPUs without

GPU support. However, future work will explore further optimizations for deployment on embedded or mobile devices.

8 REFERENCES

[1] R. Taj, F. Tao, S. Kanwal, A. Almogren, A. Altameem, and A. Ur Rehman, "A reversible-zero watermarking scheme for medical images," *Scientific Reports*, vol. 14, 2024. https://doi.org/10.1038/s41598-024-67672-9

[2] A. Al-Haj and H. Abdel-Nabi, "An efficient watermarking algorithm for medical images," *Multimedia Tools and Applications*, vol. 80, pp. 26021–26047, 2021. https://doi.org/10.1007/s11042-021-10801-7

[3] N. Sabah, N. Abbas, N. L. Emad Kadhim, and M. Majeed, "Hiding information in digital images using LSB steganography technique," *International Journal of Interactive Mobile Technologies (iJIM)*, vol. 17, no. 7, pp. 167–178, 2023. https://doi.org/10.3991/ijim.v17i07.38737

[4] M. Mehrabi, V. Zarei, and M. Ghanbari, "A highly robust medical image watermarking method for medical real-time applications," *Journal of Medical Signals & Sensors*, vol. 13, no. 3, pp. 199–199, 2023. https://doi.org/10.4103/jmss.jmss_15_22

[5] A. Amsaveni, S. Palanisamy, S. Guizani, and H. Hamam, "Next-generation secure and reversible watermarking for medical images using hybrid Radon-Slantlet transform," *Results in Engineering*, vol. 24, p. 103008, 2024. https://doi.org/10.1016/j.rineng.2024.103008

[6] S. Naima, A. Z. E. Boukhamla, Z. Narima, K. Amine, K. M. Redouane, and A. K. Sahu, "Secure and imperceptible frequency-based watermarking for medical images," *Circuits, Systems, and Signal Processing*, vol. 44, no. 1, pp. 196–217, 2024. https://doi.org/10.1007/s00034-024-02814-y

[7] Y. Fan, J. Li, U. A. Bhatti, S. A. Nawaz, and Y. Chen, "Medical image hybrid watermark algorithm based on frequency domain processing and Inception v3," *Advanced Intelligent Systems*, vol. 7, no. 6, pp. 1–13, 2025. https://doi.org/10.1002/aisy.202400654

[8] N. A. Ali and I. I. Hamid, "Watermarking in medical image," *International Journal of Online and Biomedical Engineering (iJOE)*, vol. 19, no. 6, pp. 114–126, 2023. https://doi.org/10.3991/ijoe.v19i06.37591

[9] L. Laouamer and M. Alswaili, "Hough transform-based robust informed watermarking approach for medical images," *Traitement du Signal*, vol. 41, no. 3, pp. 1557–1564, 2024. https://doi.org/10.18280/ts.410343

[10] Y. Yuan, J. Li, J. Liu, U. A. Bhatti, Z. Liu, and Y. Chen, "Robust zero-watermarking algorithm based on discrete wavelet transform and daisy descriptors for encrypted medical image," *CAAI Transactions on Intelligence Technology*, vol. 9, no. 1, pp. 40–53, 2024. https://doi.org/10.1049/cit2.12282

[11] P. Amrit, N. Baranwal, K. N. Singh, and A. K. Singh, "ConvNet-HIDE: Deep-learning-based dual watermarking for health-care images," *IEEE MultiMedia*, vol. 31, no. 3, pp. 78–87, 2024. https://doi.org/10.1109/MMUL.2024.3423370

[12] A. El Adel, M. Zaied, and C. Ben Amar, "Learning wavelet networks based on multiresolution analysis: Application to images copy detection," in *2011 International Conference on Communications, Computing and Control Applications (CCCA)*, Hammamet, Tunisia, 2011, pp. 1–6. https://doi.org/10.1109/CCCA.2011.6031444

[13] N. You, L. Han, D. Zhu, and W. Song, "Research on image denoising in edge detection based on wavelet transform," *Applied Sciences*, vol. 13, no. 3, p. 1837, 2023. https://doi.org/10.3390/app13031837

[14] M. Zaied, C. Ben Ammar, and M. A. Alimi, "Award a new wavelet based beta function," *International Conference on Signal, System and Design*, vol. 1, no. SSD03, pp. 185–191, 2003.
[15] C. Ben Ammar, M. Zaied, and M. A. Alimi, "Beta wavelets. Synthesis and application to lossy image compression," *Advances in Engineering Software*, vol. 36, no. 7, pp. 459–474, 2005. https://doi.org/10.1016/j.advengsoft.2005.01.013
[16] R. Zahmoul, R. Ejbali, and M. Zaied, "Image encryption based on new beta chaotic maps," *Optics and Lasers in Engineering*, vol. 96, pp. 39–49, 2017. https://doi.org/10.1016/j.optlaseng.2017.04.009
[17] Q. Zhang and A. Benveniste, "Wavelet networks," *IEEE Transactions on Neural Networks*, vol. 3, no. 6, pp. 889–898, 1992. https://doi.org/10.1109/72.165591
[18] R. B. Salah and M. Zaied, "A robust medical image watermarking approach using beta chaotic map, DWT, and SVD," in *2023 International Conference on Cyberworlds (CW)*, Sousse, Tunisia, 2023, pp. 201–208. https://doi.org/10.1109/CW58918.2023.00037
[19] C.-H. Un and K.-C. Choi, "Deep watermarking based on swin transformer for deep model protection," *Applied Sciences*, vol. 15, no. 10, p. 5250, 2025. https://doi.org/10.3390/app15105250
[20] N. R. M. Al_Airaji, N. I. A. Aljazaery, and H. Th. S. ALRikabi, "Adaptive HDR image blind watermarking approach based on redundant discrete wavelet transform," *International Journal of Interactive Mobile Technologies (iJIM)*, vol. 17, no. 10, pp. 136–154, 2023. https://doi.org/10.3991/ijim.v17i10.38795
[21] F. Schuch, L. Walger, M. Schmitz, and T. Rüber, "The bonn open presurgery MRI dataset of people with epilepsy and focal cortical dysplasia type II," OpenNeuro, 2023. https://doi.org/10.18112/openneuro.ds004199.v1.0.2

9 AUTHORS

Rayen Ben Salah received her Bachelor's degree in Computer Networks from the Higher Institute of Applied Sciences and Technologies of Gafsa (ISSATG) in 2014. She obtained her Research Master's degree in Business Intelligence from the same institution in 2017. She is currently pursuing a Ph.D. in Computer Science at the National Engineering School of Gabes (ENIG), Tunisia. Her research interests include image processing, computer vision, and information security, with a particular focus on robust watermarking techniques for medical imaging. She is also a member of the Research Team in Intelligent Machines (RTIM), where she contributed to projects at the intersection of artificial intelligence and health technologies (E-mail: rayen.bensalah@isimg.tn).

Mourad Zaied received his Engineering degree from the National Engineering School of Monastir in 1995. He later obtained a Master's degree (2003), a Ph.D. in Computer Engineering (2008), and the Habilitation to Supervise Research (HDR) in 2013 from the National Engineering School of Sfax, Tunisia. Since 1997, he has held various academic positions at the University of Gabes, where he is currently a Professor at the National Engineering School of Gabes (ENIG). He also leads the Research Team in Intelligent Machines Laboratory (RTIM-LAB). His research interests focus on machine learning, computer vision, and their applications in intelligent systems.